Wigner function statistics in classically chaotic systems

2003 J. Phys. A: Math. Gen. 36 4015

(http://iopscience.iop.org/0305-4470/36/14/307)

INSTITUTE OF PHYSICS PUBLISHING JOURNAL OF PHYSICS A: MATHEMATICAL AND GENERAL

J. Phys. A: Math. Gen. **36** (2003) 4015–4034 PII: S0305-4470(03)58165-3

Wigner function statistics in classically chaotic systems

Martin Horvat and Tomaž Prosen

Physics Department, Faculty of Mathematics and Physics, University of Ljubljana, Slovenia

E-mail: martin@fiz.uni-lj.si and prosen@fiz.uni-lj.si

Received 9 January 2003
Published 26 March 2003
Online at stacks.iop.org/JPhysA/36/4015

Abstract

We have studied statistical properties of the values of the Wigner function $W(x)$ of 1D quantum maps on compact 2D phase space of finite area V. For this purpose we have defined a Wigner function probability distribution $P(w) = (1/V)\int \delta(w - W(x))\,\mathrm{d}x$, which has, by definition, fixed first and second moments. In particular, we concentrate on relaxation of time-evolving quantum states in terms of $W(x)$, starting from a coherent state. We have shown that for a classically chaotic quantum counterpart the distribution $P(w)$ in the semiclassical limit becomes a Gaussian distribution that is fully determined by the first two moments. Numerical simulations have been performed for the quantum sawtooth map and the quantized kicked top. In a quantum system with Hilbert space dimension $N(\sim 1/\hbar)$ the transition of $P(w)$ to a Gaussian distribution was observed at times $t \propto \log N$. In addition, it has been shown that the statistics of Wigner functions of propagator eigenstates is Gaussian as well in the classically fully chaotic regime. We have also studied the structure of the nodal cells of the Wigner function, in particular the distribution of intersection points between the zero manifold and arbitrary straight lines.

PACS numbers: 03.65.Yz, 03.65.Sq, 05.45.Mt

(Some figures in this article are in colour only in the electronic version)

1. Introduction

The Wigner function (WF) [1] is an essential concept of the phase-space representation of quantum mechanics, namely it is a useful and faithful representation of a pure or mixed quantum state in terms of functions of canonical classical phase-space variables. It has many applications in various branches of physics, in particular in quantum optics. However, the WF cannot be interpreted as a quantum phase-space distribution as it can develop negative values, in particular due to the well-known oscillatory interference fringes following, e.g., coherent wave-packet superpositions.

The WF also played an important role in the realm of quantum chaology [2, 3]. In particular, it has been conjectured that the WF of stationary eigenstates of bounded dynamical systems in quasi-classical regimes localizes onto classically invariant components of phase space. For example, for classically regular phase-space regions, such as KAM tori, the WF is supposed to become a Dirac delta function on a KAM torus whereas for a classically chaotic component the WF is supposed to condense uniformly there. However, it is well known that this asymptotic behaviour is to be understood in a very weak limit sense, i.e. the WF is becoming uniform only after being integrated (with a very smooth test function) over a non-small (or classical) region of phase space. On the other hand, on a smaller (quantum) scale, e.g., of Planck cell size, the phase-space structure of the WF of typical, say random or ergodic states, is very much unknown. This question is important for the understanding of decoherence and quantum stability with respect to system perturbations as discussed recently [4–7].

In this paper, we address the question of the structure of a typical WF from a statistical point of view. We define and analyse the statistical distribution of values of the WF of a given quantum state. In particular, we are interested in the relaxation of this distribution with time, when we start from an initial coherent state, and in the corresponding time scale. Here we limit ourselves to classically fully chaotic and discrete time systems, namely the chaotic quantum maps, where the full phase space is the only topologically transitive ergodic component.

We show that for chaotic quantum maps, the limiting WF value distribution is a Gaussian. The average value is fixed by normalization, while the second moment (or the variance) diverges in the quasi-classical limit ($\hbar \to 0$), so we have roughly a symmetric distribution of positive and negative values of the WF for random states. In addition, we show that for chaotic systems, the relaxation to equilibrium in statistics of the WF happens on a short $\log \hbar$ (Ehrenfest) time scale. Furthermore, we show for chaotic systems, that the statistics of the WF of a typical chaotic eigenstates is the same as the WF statistics of a random state, which is consistent with the established Berry's conjecture [20]. Finally, we present statistical analysis of the structure of nodal cells of the WF of chaotic or random states and show that it can be described by simplified models based on random trigonometric functions.

In section 2, we outline the essentials of the general Wigner–Weyl formalism and discuss two special cases of compact phase space, namely of toroidal and spherical phase space, which are later used in numerical examples. In section 3 we discuss the WF value statistics of a random (or quantum chaotic) state. In section 4 we discuss WF statistics on two numerical examples of quantum chaos, and analyse, in particular, the relaxation of WF statistics in quantum time evolution starting from an initial coherent state. In section 5 we go beyond simple value statistics, and study also the phase-space structure statistics of the WF, such as its spatial correlation function and distribution of diameters of its nodal cells, for example. In section 6 we summarize our most important results and conclude.

2. Weyl–Wigner formalism and the Wigner function

Let us first review some of the essential general principles of the Weyl–Wigner (WW) phase-space representation of operators (see, e.g., [8]). As we are aiming at compact (finite) phase spaces of chaotic maps, our discussion of the WW formalism has to be a little bit abstract so as to be able to incorporate the different topologies that are discussed later. We begin by considering a phase space χ and a Hilbert space $\mathcal{H}$, such that a typical function $A(x)$, $x \in \chi$, corresponds under quantization to a linear operator $\hat{A}$ over $\mathcal{H}$. The inverse map $\hat{A} \to A(x)$ is called a Weyl symbol, and if $\hat{A} = |\psi\rangle\langle\psi|$ then the corresponding symbol is called the WF. The Weyl symbol can be formally constructed using a self-adjoint kernel operator $\hat{\omega}(x)$ with

the property

$$\mathrm{tr}\{\hat{\omega}(x)\hat{\omega}(y)\} = \delta(x-y) \qquad \hat{\omega}(x)^{\dagger} = \hat{\omega}(x) \tag{1}$$

namely

$$A(x) = \mathrm{tr}\{\hat{\omega}(x)\hat{A}\} \tag{2}$$

which also generates the inverse map

$$\hat{A} = \int \mathrm{d}V\, A(x)\hat{\omega}(x). \tag{3}$$

For systems with classically compact (finite) phase space χ the corresponding Hilbert space is finite, say N dimensional. As a consequence, the WW map (2) can be uniquely inverted only if the phase space is restricted to a finite set of N^2 points $\chi' = \{x_{nk}; n, k = 0, 1, \ldots, N-1\}$. The kernel is in this case defined at discrete points only, $\hat{\omega}_{nk} = \hat{\omega}(x_{nk})$ with the property

$$\mathrm{tr}\{\hat{\omega}_{nk}\hat{\omega}_{ml}\} = \delta_{nm}\delta_{kl} \tag{4}$$

so that the discrete WW map reads

$$A_{nk} = \mathrm{tr}\{\hat{\omega}(x_{nk})\hat{A}\} \qquad \text{and} \qquad \hat{A} = \sum_{nk} A_n \hat{\omega}_{nk}. \tag{5}$$

The WF $W(x)$ is defined as a phase-space representation of the density operator $\hat{\rho}$ multiplied by a certain suitable normalization constant C

$$W(x) = C\,\mathrm{tr}\{\hat{\omega}(x)\hat{\rho}\}. \tag{6}$$

The constant C can be set for the convenience of a particular application, for example, usually it is set by the normalization of probability, $\int \mathrm{d}x\, W(x) = 1$. However, in this paper we are interested in the fluctuation of the WF so we determine the constant C by fixing the standard deviation $\sigma^2 = \overline{W^2} - \overline{W}^2 = 1$, where $\overline{(\cdots)}$ denotes the average over phase space. We note that the kernel $\hat{\omega}$ is far from being completely specified by the property (1). In addition we need certain correspondence principles. For example, for the usual (non-compact) symplectic geometry $x = (q, p)$ in $(d+d)$-dimensional phase space the kernel reads $\hat{\omega}(q, p) = (2\pi\hbar)^{-d/2} \int \mathrm{d}v\, \mathrm{e}^{\mathrm{i}p\cdot v/\hbar} |q + v/2\rangle\langle q - v/2|$. However, for compact geometries the WW map may not be unique. In such cases one may decide on the most reasonable or the simplest choice. In any case, as the effective value of Planck constant vanishes any consistent choice should yield equivalent results in the semiclassical limit.

2.1. Wigner function on a 2D torus

Many simple phenomena in the theory of bounded Hamiltonian (symplectic) dynamical systems can be demonstrated on a 2D torus $\chi = T^2 = [0, 2\pi) \times [0, 2\pi)$. However, quantization of a torus is not trivial from a mathematical point of view. Hence there are several different proposals for a WW formalism on a torus [15]. Here we are following [11] up to convenient scaling factors. Let the Hilbert space $\mathcal{H}$ have dimension N, and the canonical bases, namely the position basis $|n\rangle$, $n = 0, \ldots, N-1$, and the momentum basis $|\tilde{k}\rangle$, $k = 0, \ldots, N-1$, satisfy $\langle n|\tilde{k}\rangle = N^{-1/2}\exp(-2\pi\mathrm{i}nk/N)$. The *quantum phase space* in our formalism is a discrete mesh of $N \times N$ points, $x_{nk} = (2\pi n/N, 2\pi k/N)$. The WF function on such a discrete phase space in the limit of $N \to \infty$ mimics the continuous Wigner function [1]. For technical reasons we assume that N is *odd*. The WW kernel in this formalism is defined as

$$\hat{\omega}_{nk} = \frac{1}{\sqrt{N}} \sum_{n'l} \exp(-2\pi\mathrm{i}n'k/N)\tilde{\delta}(2l - 2n + n')|l\rangle\langle l + n'|$$

where all indices run from $-(N-1)/2$ to $(N-1)/2$, which will be assumed whenever we refer to the quantized torus. For a pure quantum state ψ the WF is given by

$$W_\psi(n,k) = C_t \,\mathrm{tr}\{\hat{\omega}_{nk}\hat{\rho}\} \qquad C_t = \sqrt{\frac{N^3}{N-1}}$$
$$= \frac{N}{\sqrt{N-1}} \sum_{n',l} \exp[-2\pi \mathrm{i} n'k/N]\tilde{\delta}(2l-2n+n')\langle l+n'|\psi\rangle\langle\psi|l\rangle \tag{7}$$

where we define a fat Dirac delta function $\tilde{\delta}(l)$ as

$$\tilde{\delta}(l) = \frac{1}{N}\sum_{m'} \exp(\pi \mathrm{i} m' l/N) = \frac{1}{N}\frac{\sin(\pi l/2)}{\sin(\pi l/2N)}.$$

2.2. *Wigner function on a sphere*

As a second important special case we consider the quantum mechanics of a spin J variable whose classical phase space can be identified with a unit sphere $\chi = S^2$ described by spherical angles $\theta \in [0,\pi)$, $\varphi \in [0,2\pi)$. The WW formalism for $SU(2)$ geometry was developed in [14] with the kernel

$$\hat{\omega}(x) = \sum_{kq} \hat{T}_{kq} Y^*_{kq}(x) \qquad x = (\theta,\varphi)$$

where Y_{kq} are standard spherical harmonics and $\hat{T}_{kq}$ are multipole operators defined by

$$\hat{T}_{kq} = \sum_{m=-J}^{J}\sum_{m'=-J}^{J} (-1)^{J-m}\sqrt{2k+1}\begin{pmatrix} J & k & J \\ -m & q & m' \end{pmatrix}|Jm\rangle\langle Jm'|.$$

Symbols $\left(\begin{smallmatrix} J & k & J \\ -m & q & m' \end{smallmatrix}\right)$ are standard Wigner $3j$ symbols [17]. Using the kernel one defines the WF as [12]

$$W(x) = C_s \,\mathrm{tr}\{\hat{\omega}(x)\hat{\rho}\} = C_s \sum_{k=0}^{2J}\sum_{q=-k}^{q=k} G_{kq} Y_{kq}(x) \qquad C_s = \sqrt{4\pi\frac{2J+1}{2J}}. \tag{8}$$

The information about the quantum system state-density operator $\hat{\rho}$ is hidden in the coefficients

$$G_{kq} = \mathrm{tr}\left\{\hat{\rho}\hat{T}^\dagger_{kq}\right\}.$$

We note that the $SU(2)$ WF is defined continuously everywhere on a sphere. However, it is a superposition of *finitely* many spherical functions with coefficients G_{kq} which correspond to a discrete WF over a finite discrete mesh of points on some other compact geometries, such as a torus.

3. Wigner function value statistics of a random state

Quantum states of classically chaotic systems are usually associated with the so-called *ergodic* or *random* wavefunctions. These random states can be constructed using very simple principles, such as Berry's random plane wave superposition for billiards [20], or chaotic analytic functions in the Bargman or Husimi representation of Hannay [9], see also [10]. In this paper we want to analyse the Wigner function of a random state and its statistical properties. To the best of our knowledge this has not been attempted before.

Starting from a fixed WF $W(x)$ we define its value distribution $P(w)$ as

$$P(w) = \frac{1}{V}\int_{\chi} \delta(w - W(x))\,\mathrm{d}x. \tag{9}$$

We assumed that phase space χ is compact and has finite volume V. The averages with respect to the probability density $P(w)$ will be denoted by $\overline{(\cdots)}$. The first moment of $P(w)$ is fixed by normalization of the Wigner function (given by constant C'). The second moment is also fixed by the purity of the state which implies

$$\int \mathrm{d}x\, W^2(x) = C' \int \mathrm{d}x\, W(x). \tag{10}$$

Since in this paper we are interested in fluctuation of the WF it is convenient to determine the scaling constant C' (6) by setting the standard deviation to one, $\sigma^2 = \overline{W^2} - \overline{W}^2 = 1$. This implies for the average values (first moments), using equations (7), (8):

$$\text{torus:}\quad \overline{W} = \frac{1}{\sqrt{N-1}} \qquad \text{sphere:}\quad \overline{W} = \frac{1}{\sqrt{2j}}. \tag{11}$$

It may be instructive to define a *relative standard deviation* in units of the average WF $\kappa = \sigma/\overline{W}$. Then the above statement (11) says that the relative standard deviation $\kappa \to \infty$ of the WF distribution *diverges* in the semiclassical limit $N \to \infty$ (or $j \to \infty$).

We should note that the result on divergence of the relative standard deviation is general and independent of the structure of the state. So, if we have a very non-uniform state, e.g., a Gaussian wave packet, then the statement says merely that the standard deviation is very large compared to the average value since we have almost all density concentrated around a small region. However, if we have a random (ergodic) state, then the WF value distribution should be transitionally invariant in phase space. Therefore, the values of the first two moments of the global phase space WF value distribution should also determine the average and standard deviation of the local distribution around each phase-space point. In order to determine the entire WF value distribution we define an appropriate random WF model in a specific generic geometry, namely on a 2D torus, although the result which will be obtained can be argued to be universal and geometry independent. We start with a random state in N-dimensional Hilbert space

$$|\psi\rangle = \sum_{l=1}^{N} c_l |l\rangle \qquad \sum_{l=1}^{N} |c_l|^2 = 1 \tag{12}$$

where c_l are random generally complex coefficients. It turns out (see, e.g., [19]) that for large N, coefficients c_l may be considered as independent complex Gaussian variables with variance $\langle |c_l|^2 \rangle = 1/N$ (here and later $\langle \cdots \rangle$ denotes averaging over an ensemble of random states (12)).

Translational invariance of the WF value distribution implies that the distribution over phase space can be replaced with the distribution over an ensemble of random states (12), so we choose to study the distribution of WF at the most easily computable phase-space point (0, 0)

$$W_{00} = \frac{N}{\sqrt{N-1}} \left(|c_0|^2 + \sum_{l \neq l'} \tilde{\delta}(l + l') c_l^* c_{l'} \right). \tag{13}$$

In the leading order $\tilde{\delta}(l + l')$ can be approximated by the Kronecker $\delta_{l+l'}$ so expression (13) is a sum of N independent terms, the first $|c_0|^2$ is strictly non-negative, while the others have

vanishing mean and finite fluctuation. Hence, due to the central limit theorem, for large $N \gg 1$, the distribution of W_{00} becomes Gaussian

$$P(w) = \frac{1}{\sqrt{2\pi}} \exp\left(-\frac{1}{2}(w - \overline{W})^2\right) \tag{14}$$

where the first and second moments can be computed directly by ensemble averaging giving identical results to previous phase averaging (11), and $\sigma^2 = 1$.

4. Dynamics and relaxation of Wigner function value statistics

In this section we will consider dynamics, namely statistics of the WF of time-evolving pure states. In particular, we shall focus on systems with ergodic, mixing, and fully chaotic classical dynamics such that in the course of classical dynamics any non-singular initial classical measure relaxes to a uniform (micro-canonical) measure. When turning to quantum mechanics we pose a simple problem. Let us start with 'the most classical' initial state, namely with the coherent state (e.g., Gaussian wave packet): First, how does the WF value distribution of a time-evolving state relax into the Gaussian distribution (14) which characterizes the final ergodic (random) state? Second, what is the characteristic time scale of this relaxation process for a typical chaotic system and how does it scale with the value of an effective Planck constant?

4.1. Toy models of quantum chaotic dynamics

In order to carry out the plan outlined above we need to define generic time evolution on the Hilbert spaces of the quantized torus or the quantized sphere, respectively, which are chaotic in the classical limit. This is not difficult as we simply consider popular models which have been widely studied in the literature, namely the quantized sawtooth map on the torus [18], and the quantized kicked top [19].

The quantized sawtooth map on the torus (the classical counterpart is defined on a torus $(q, p) \in [0, 2\pi] \times [0, 2\pi L]$) defined on the finite Hilbert space of dimension N with the evolution operator

$$\hat{U}_s = \exp\left(-\mathrm{i}\frac{T}{2}\hat{m}^2\right) \exp\left(\mathrm{i}\frac{K_0 T}{2L^2}\hat{n}^2\right) \tag{15}$$

where K_0 is the kicking strength, $T = 2\pi L/N$ is the period of forcing and integer L (usually set to 1) measures the vertical size of toroidal phase space. We have introduced formal position and momentum operators with integer eigenvalues, namely $\hat{n}$ and $\hat{m}$ respectively, satisfying $\hat{n}|n\rangle = n|n\rangle, \hat{m}|m\rangle = m|m\rangle$. We should note that the classical sawtooth map is ergodic and uniformly hyperbolic for $K_0 > 0$. As for the initial state we always choose a coherent state (which can be expressed in terms of Jacobi theta functions for toroidal phase space [16]) centred somewhere on the torus.

As for the other system defined (classically) on a spherical phase space, the quantum kicked top of spin J has a unitary map $\hat{U}_k$ acting on a $(2J + 1)$-dimensional Hilbert space

$$\hat{U}_k = \exp(-\mathrm{i}\gamma \hat{J}_x) \exp\left(\mathrm{i}\alpha \hat{J}_z^2 / 2J\right).$$

Here, parameter α is an angle of rotation in between the kicks and γ is the kicking strength. In the paper we will consider the parameter values $\gamma = \pi/2$ and $\alpha = 3$, or $\alpha = 10$, corresponding to classically mixed, or fully chaotic, phase space, respectively. Again, we prepare the system initially in the $SU(2)$ coherent state [13] placed somewhere on the sphere.

For the purpose of illustration we first show the cascade of snapshots of WF starting from the initial coherent state undergoing quantum dynamics with completely chaotic classical time evolution. The results are shown in figure 1 for the quantized sawtooth map while similar-looking cartoons were obtained for the kicked top. It is clear from the figure that after a very short time (of the order of a few kicks) the Wigner function relaxes into a universal looking distribution with a roughly symmetric distribution of positive and negative values. We conjecture that this asymptotic distribution should be a Gaussian (14) as derived for a random model. Furthermore, we conjecture that the time scale on which this relaxation takes place is just of the order of the so-called Ehrenfest time [24], that is the time needed for the initially localized wave packet to spread over the accessible phase space $t_{\rm ehr} = \log \hbar/\lambda$ where λ is a classical Lyapunov exponent.

4.2. Wigner function value distribution

Firstly, we want to check the relaxation of the WF value statistics $P(w)$ starting from the initial coherent state. Using numerical experiments with the sawtooth map and the kicked top we confirm our expectation and obtain fast relaxation into statistically significant Gaussian distribution (14). The cascade of distributions $P(w)$ for several consecutive kicks in the sawtooth map is shown in figure 2. It is perhaps interesting to note that the relaxation goes through an intermediate distribution which seems to have exponential tails (see a snapshot of the 10th kick). A very similar result is also obtained for the kicked top model shown in figure 3(a). For comparison we show in figure 3(b) stationary WF value distributions obtained from time evolution starting from a random state. In this case we obtain, as expected, for the initial state, and for time-evolving states, a nice agreement with a Gaussian WF value distribution.

4.3. Relaxation time scale

Secondly, we want to quantitatively characterize the deviations from Gaussian statistics and thus to measure the time scale of relaxation. To this end we define the excess ϵ of the WF value distribution $P(w)$

$$\epsilon = \overline{(w - \overline{W})^4}/\sigma^4 - 3. \tag{16}$$

Note, that $\epsilon = 0$ for a Gaussian (14) and the size of ϵ should roughly measure the deviation from a Gaussian. As we have discussed above, we expect the relaxation process to take place within the Ehrenfest time scale

$$t_{\rm r} \sim \log N/\lambda \tag{17}$$

where λ is an effective (average) Lyapunov exponent and N is the dimensionality of Hilbert space. This is certainly a lower bound to a relaxation time scale, but as we will show by numerical experiments, it also gives the right scaling and order of magnitude of the true relaxation time. For this purpose we choose only the quantized sawtooth map where much larger N is accessible so that the logarithmic scaling can be checked.

In figure 4 we plot ϵ as a function of time of the WF value distribution starting from coherent initial states, for different values of N over several orders of magnitude. Indeed we observe a very clean transition from $\epsilon \approx 0.65$ to $\epsilon = 0$ at around $t \approx \log N$. In order to also check the dependence on the Lyapunov exponent $\lambda(K_0)$ we have plotted in figure 5 the relaxation of excess ϵ for several different values of chaoticity parameter K_0 and fixed N. We have found that the transition time scale is proportional to λ^{-1} therefore supporting formula (17).

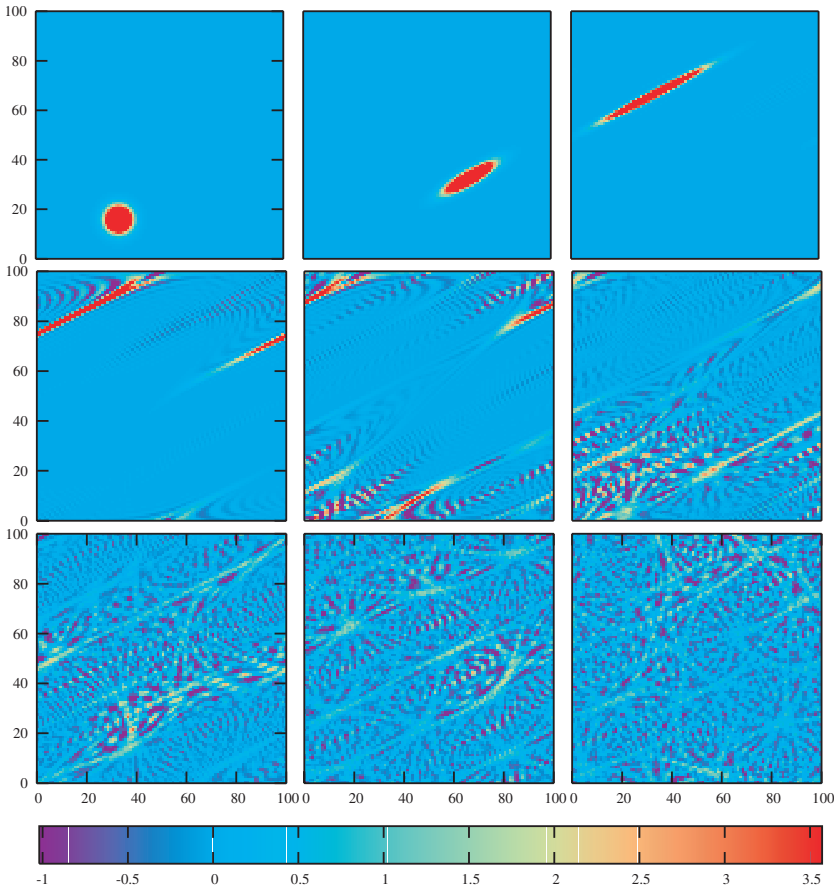

Figure 1. The dynamics of the WF in the quantized sawtooth map for parameters $K = 0.5$, $L = 1$ and dimension $N = 101$. The system is initially in the coherent state centred at $(q, p) = (\frac{2}{3}\pi, \frac{1}{3}\pi)$. The WF at successive integer time steps is shown from left to right and from top to bottom. The colour code bar of the Wigner function values is shown at the bottom of the figure. Note the significant contribution of negative values for longer times.

Since ϵ is only one number which cannot characterize the overall distribution $P(w)$ we have made the following additional check. We know that for a random state in the limit $N \to \infty$ the probability of having a negative value of the WF goes to $1/2$. Therefore, we propose to study the percentage of phase space with negative valued WF

$$P_- = \int_{-\infty}^{0} P(w)\,\mathrm{d}w \tag{18}$$

as a function of time. The results of numerical experiment for the quantized sawtooth map are shown in figure 6. We see that P_- converges very fast to $1/2$ on a time scale (t_c) proportional to $\log(N)$ but significantly (around a factor of two) smaller than the relaxation time t_r. We note that negative values of WF mean serious deviation from classical Liouville density, so our result indicates that quantum–classical correspondence breaks significantly before the WF value distribution becomes actually close to a Gaussian. However, both time scales have the same scaling with N and λ.

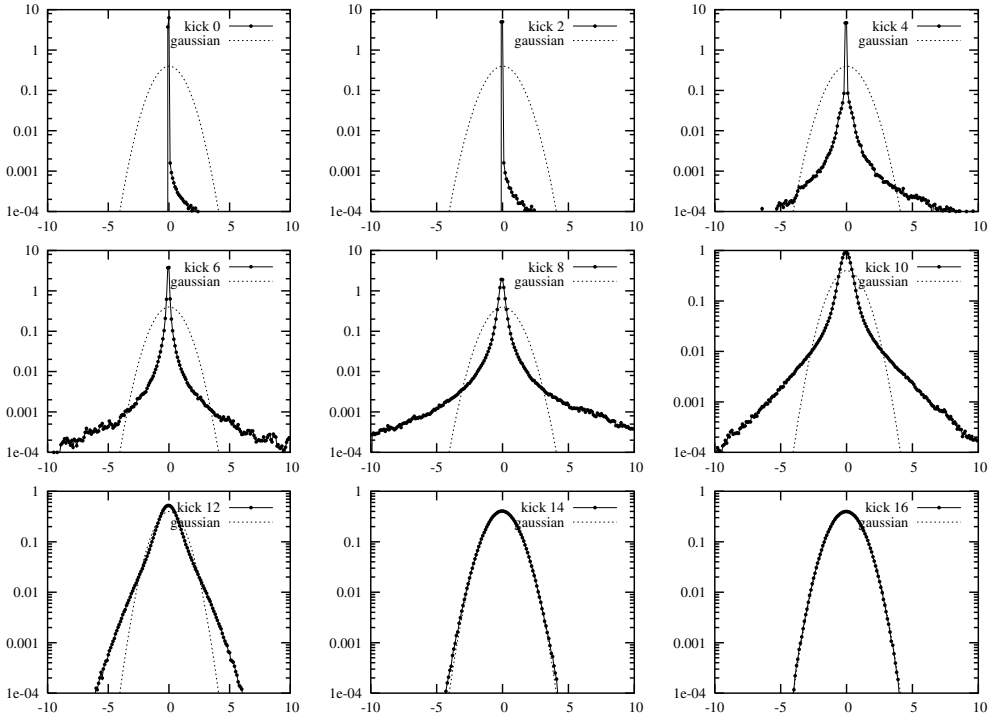

Figure 2. Time evolution of the Wigner function value distribution (9) of the quantized sawtooth map for $K_0 = 0.5$, $L = 1$ and $N = 2187$. The initial state is a coherent wave packet. Dashed curves give a theoretical Gaussian (14).

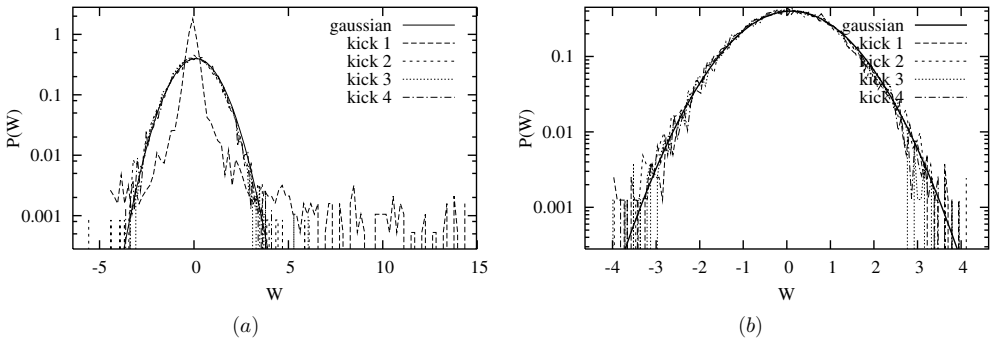

Figure 3. Time evolution of the Wigner function value distribution (9) of the quantized chaotic kicked top for $\alpha = 10$, $\gamma = \pi/2$ and $J = 50$. In (*a*) we take an initial coherent state whereas in (*b*) we take an initial random state. Consecutive kicks are shown with different line styles and the full curve is a theoretical Gaussian (14)).

4.4. Value statistics of Wigner functions of stationary eigenstates

We note that the time evolution of a Wigner function of an initial state

$$|\psi\rangle = \sum_k a_k |\psi_k\rangle \qquad a_k \in \mathbb{C} \quad \sum_k |a_k|^2 = 1 \tag{19}$$

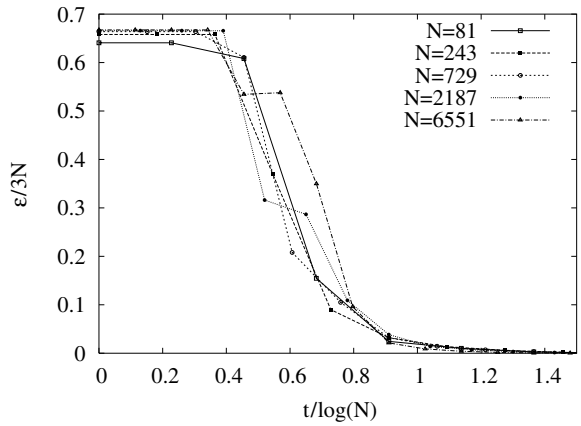

Figure 4. Scaling of relaxation to Gaussian statistics in the quantized sawtooth map, $K_0 = 0.5, L = 1$, measured with the excess ϵ of the distribution. The initial state is a coherent wave packet. Different dimensions N are indicated in the figure.

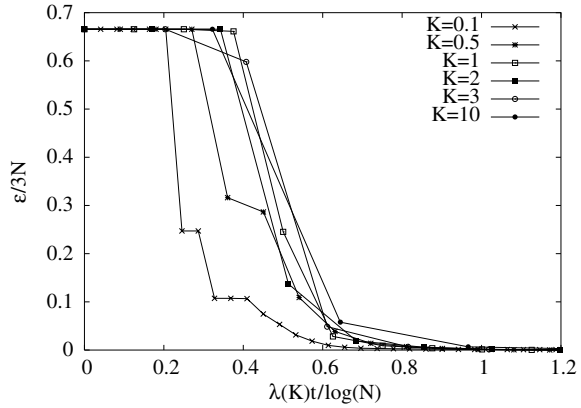

Figure 5. Excess ϵ as a function of time for the quantized sawtooth map at different kicking strengths K_0 (see figure) and at fixed dimension $N = 2187$ and at $L = 1$. The Lyapunov exponent is given by the formula: $\lambda(K_0) = \log((2 + K_0 + ((2 + K_0)^2 - 4)^{1/2})/2)$ [18].

can be written as

$$W(x,t) = \sum_{kl} a_k a_l^* \exp(\mathrm{i}t(\Omega_k - \Omega_l)) W_{kl}(x) \qquad W_{kl}(x) = C\,\mathrm{tr}\{\hat{\omega}(x)|\psi_k\rangle\langle\psi_l|\} \tag{20}$$

in terms of the Wigner function basis W_{kl} if $|\psi_k\rangle$ are eigenfunctions of the propagator $\hat{U}^t$ with eigenvalues $\exp(\mathrm{i}t\Omega_k)$. Therefore, stationary (or time averaged) properties of a WF $W(x,t)$ are determined by the diagonal functions W_{kk}, which are the usual WF of the eigenstates of U. It is, therefore, clear that for classically chaotic and ergodic systems one should expect *almost all* $W_{kk}(x)$ to have the property of a WF of a random state. In order to confirm this conjecture we have computed the ϵ_k of the WF value distribution of a complete set of eigenfunctions $\{W_{kk}(x), k = 1, 2, \ldots\}$ and analysed its distribution. Indeed we found, as shown in figure 7 for the quantized kicked top, that in the classically chaotic case almost all eigenfunctions have $\epsilon \approx 0$. This has been further quantitatively compared to random matrix theory by computing the excess distribution for Wigner functions of eigenvectors of a Gaussian orthogonal (GOE)

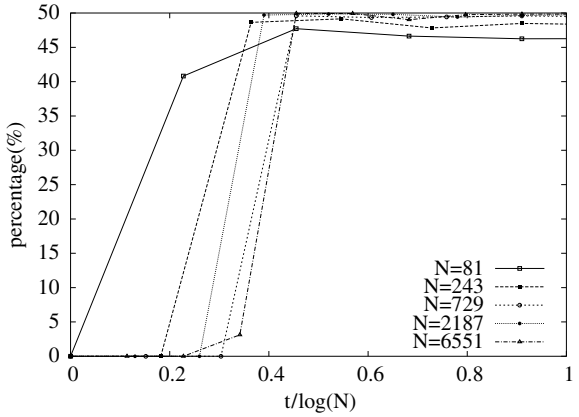

Figure 6. Percentage of phase space with negative WF as a function of scaled time for the quantized sawtooth map, $K_0 = 0.5$, $L = 1$ at several different dimensions N as indicated in the figure.

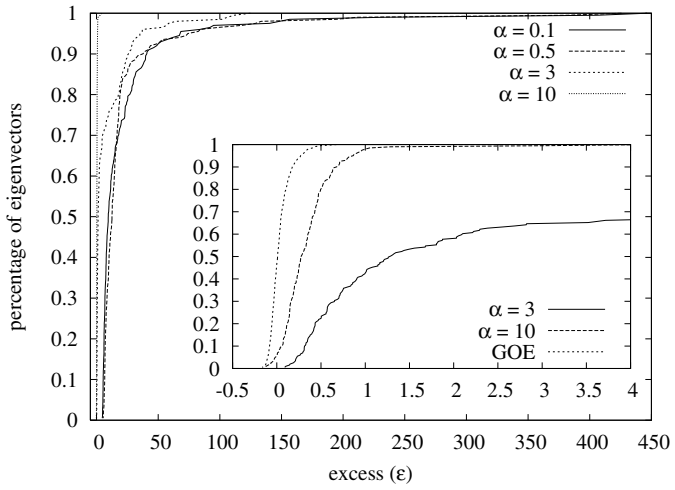

Figure 7. Cumulative distribution of the excess ϵ of the quantum kicked top eigenfunctions in the case of classically (almost) regular ($\alpha = 0.1, 0.5$), mixed ($\alpha = 3$) and fully chaotic ($\alpha = 10$) dynamics. To compare the classically chaotic case with random matrix theory, the result for GOE random matrix eigenfunctions is given in the inset on a blown up scale.

random matrix. Indeed very nice agreement was found, meaning that also the number of Wigner functions with larger excess ('accidental scars') is within the statistical fluctuation predicted by random matrix theory. In the same figure we also analyse excess distribution for mixed and regular classical dynamics, where the excess distribution has a nontrivial shape.

4.5. Auto-correlation of the Wigner function

Statistical description of the WF at individual points in phase space is meaningful if statistical correlations between Wigner function values at different phase-space points are small. Therefore, it may be interesting to define and study the auto-correlation function of the

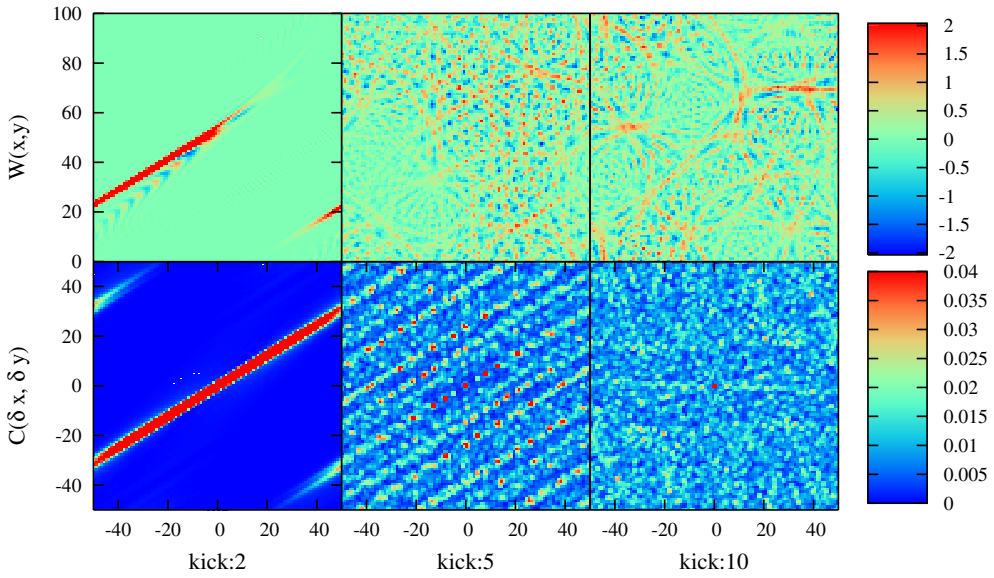

Figure 8. The density plot of auto-correlation $C(\delta x, \delta y)$ (below) and Wigner function $W(x, y)$ (above) in time evolution of the sawtooth map at dimension $N = 101$ and $K_0 = 1$, $L = 1$.

Wigner function, defined as

$$C(\delta x) = \frac{1}{V}\int W(x)W(x+\delta x)\,\mathrm{d}x \qquad \text{(continuous phase space)}$$

$$C(\delta n, \delta m) = \frac{1}{N^2}\sum_{nm} W_{nm}W_{n+\delta n,m+\delta m} \qquad \text{(discrete phase space)}.$$

The dynamics of the auto-correlation and the corresponding Wigner function starting from the coherent state placed at $(q = 2.1, p = 1.2)$ of the quantized sawtooth are shown in figure 8. At small times, when the Wigner function still has a clear non-random structure, the auto-correlation varies strongly with the displacement vector $\delta x = (\delta m, \delta n)$. From the auto-correlation function one can clearly observe the directions of stable and unstable classical flow. At later times $C(\delta x)$ becomes isotropic, and apart from the delta spike at the origin $\delta x = 0$, equals a constant, namely $C(\delta x) \sim \delta(\delta x) + \text{const}$. Indeed, for a random state we shall proceed to determine $C(\delta x)$ exactly.

We assume a random wave hypothesis, namely that a random (time-dependent) state can be written as $|\psi\rangle = \sum_n c_n|n\rangle$, where c_n are Gaussian random independent complex coefficients, satisfying $\langle c_n^* c_m\rangle = \delta_{nm}$, $\langle c_n c_m\rangle = 0$, where $\langle\cdots\rangle$ represents the average over an ensemble of states, or equivalently, a time average with a random initial state. The auto-correlation function can thus be expressed as

$$C(\delta n, \delta m) = \frac{N}{N-1}|\alpha(\delta n, \delta m)|^2 \qquad \alpha(\delta n, \delta m) = \sum_l \exp(-\mathrm{i}2\pi l\delta m/N)c_l c^*_{l+\delta n}. \tag{21}$$

Averaging over Gaussian random variables c_n can be performed straightforwardly, yielding

$$\langle C(\delta n, \delta m)\rangle = \frac{N}{N-1}\delta_{\delta n,0}\delta_{\delta m,0} + \overline{W}^2.$$

This theoretical prediction is in good agreement with numerical experiment, as shown in figure 9. We also estimate (temporal) fluctuations of $C(\delta x \neq 0)$ by standard deviation

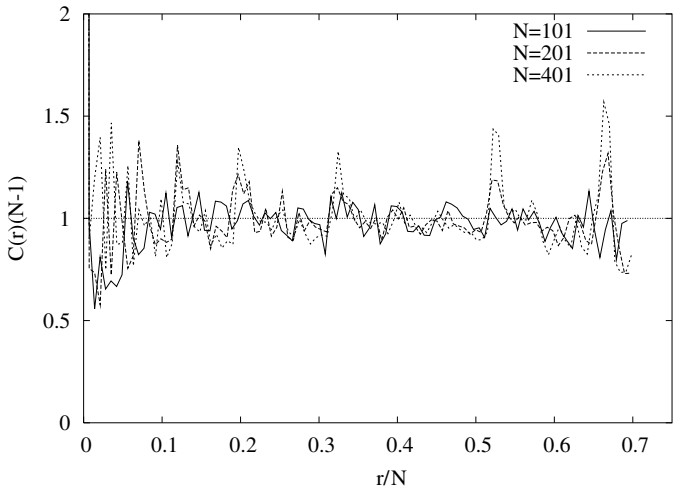

Figure 9. Scaled local time average auto-correlation function $\overline{C}$ versus the radial distance $r = \sqrt{(\delta x)^2 + (\delta y)^2}$ for different dimensions N of the quantized sawtooth map for $K_0 = 1$ and $L = 1$.

$\sigma_C^2 = \langle C^2 \rangle - \langle C \rangle^2$, which can be computed directly using Wick pair contractions in the variables c_n

$$\sigma_C = \langle C \rangle = \frac{1}{N-1} = \overline{W}^2 \qquad \text{if} \quad (\delta n, \delta m) \neq 0$$

in the asymptotic regime of high dimension $N \gg 1$.

5. Wigner function phase-space structure statistics

In previous sections we have been investigating the value statistics of the Wigner function. The WF possesses hills and valleys as compared to the reference 'altitude'—offset. Here we discuss 2D compact phase space where these structures are supported by 2D nodal cells, that in general have very rich topology. The nodal cell sizes, especially the sub-Planck size structures, have recently been brought in the connection with decoherence [4, 22]. We are now interested in the statistical properties of WF phase-space structures such as the nodal cell size and the amplitude of oscillations (hills and valleys) from a given offset value. For the offset we choose the phase-space mean value of WF (offset $= \overline{W}$) as this seems to be the most natural choice. However, since the relative mean value divided by the fluctuation goes to zero, $\overline{W}/\sigma_W \to 0$ in the limit $N \to \infty$, we argue that the results are asymptotically just the same as if one considers nodal cells with respect to zero offset.

In this work we would like to obtain some general results on WF nodal cell statistics of random (or chaotic) states. In our numerical analysis we consider time-evolving states, starting from an initial coherent state, for times $t > t_E$, when the statistics is stationary and the structure of the state is expected to be the same as that of a random state.

In order to simplify the picture we have considered the statistical properties of intersections between nodal cells (bounded by the curves $W(x) - \overline{W} = 0$) and some arbitrary (random) straight lines in phase space, i.e. we consider one-dimensional projections of two-dimensional WF. Let the straight line $R(t) \in \chi$ be parametrized by a real variable t. In the case of spherical phase space, the set of all straight lines consists of all great circles, while in the case of toroidal

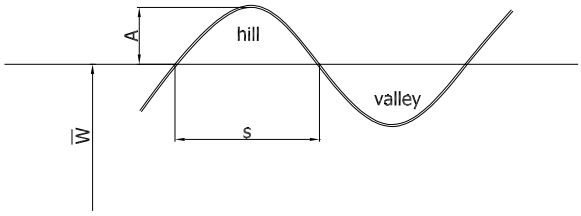

Figure 10. The sketch of 1D phase-space structures of the intersected WF.

phase space we consider for simplicity only closed straight lines, i.e. the two sets of irreducible circles specified by either fixing position or fixing momentum.

The central object studied here is the so-called Wigner function on a line (abbreviated WFL) with an offset value subtracted and assuming that the circumference of the circle is equal to 2π:

$$\widetilde{W}_{\psi,R}(t) = W_\psi[R(t)] - \overline{W} \qquad R(t) \in \chi \quad t \in [0, 2\pi]. \tag{22}$$

Since the statistical properties of a Wigner function of a random or ergodic quantum state are invariant under phase-space translations, the parameters of the line (circle) $R(t)$ can also be chosen as random. In other words one may average over lines $R(t)$ in a uniform way, such that an ensemble of lines $R(t)$ uniformly covers the phase space with respect to an ergodic invariant measure. We shall investigate the following statistical distributions defined with respect to $W_{\psi,R}(t)$: (i) distribution $\mathrm{d}\mathcal{P}(s)/\mathrm{d}s$ of spacings $s = t_{n+1} - t_n$ between adjacent zeros t_n of $W_{\psi,R}(t)$ which may also be called the 'diameter distribution of Wigner nodal cells', (ii) distributions of amplitudes $\mathrm{d}\mathcal{P}(A)/\mathrm{d}A$, i.e. local maxima (hills) and local minima (valleys) between each pair of adjacent zeros as illustrated in figure 10 and (iii) joint distribution of spacings s and the corresponding amplitudes A, $\mathrm{d}\mathcal{P}(s, A)/\mathrm{d}s\,\mathrm{d}A$.

5.1. Random model of a Wigner function on a line

We would like here to propose a simple statistical model which reproduces the properties of a random Wigner function on a line. We start by a simple ansatz expanding the WFL into the Fourier modes

$$\widetilde{W}(t) = u_0 + \sum_{q=1}^{M} u_q \cos(qt) + v_q \sin(qt) \tag{23}$$

where coefficients u_q and v_q are some Gaussian (asymptotically, as $N \to \infty$, statistically independent) random variables with zero mean $\langle u_q \rangle = 0$, $\langle v_q \rangle = 0$ and prescribed variances $\langle u_q^2 \rangle = O(N^{-1})$, $\langle v_q^2 \rangle = O(N^{-1})$. The effective number of Fourier modes M is usually of the same order as the dimension of the Hilbert space N. The ansatz (23) shall be proved separately for the case of a WF on the torus and on the sphere, and also the expressions for the variances of coefficients u_n and v_n shall be computed. We will then use our statistical model to compare with exact numerical calculations in our two model systems.

5.1.1. Random model on the torus. We expect the statistical structure of a random WF to be the same in both the simplest sets of directions, namely for fixed position or fixed momentum. We limit the analysis which follows to the circles of fixed position. We start from a 'random'

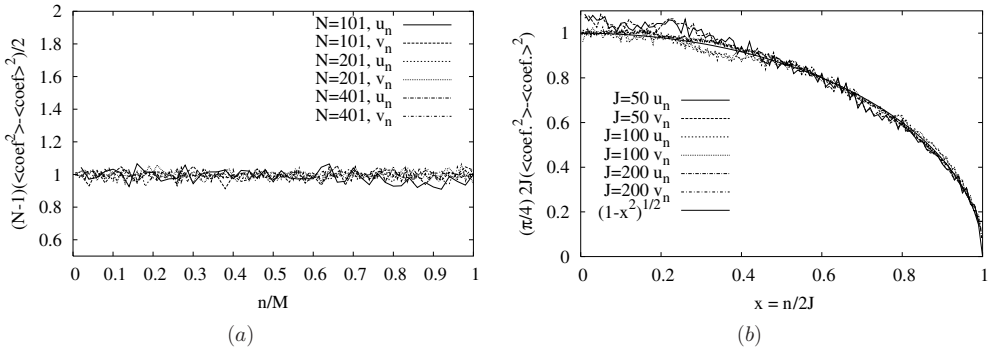

Figure 11. Variances of the Fourier coefficients of the WFL of a random state: (*a*) in the case of toroidal phase space, and (*b*) in the case of spherical phase space.

state written in the position basis $\{|n\rangle\}_{n=1,\dots,N}$ of the Hilbert space of dimension N, as

$$|\psi\rangle = \sum_{n=0}^{N} c_n |n\rangle \qquad c_n \in \mathrm{C} \tag{24}$$

with uncorrelated complex Gaussian coefficients (in the asymptotic regime $N \to \infty$) specified by

$$\langle c_n \rangle = 0 \qquad \langle c_m^* c_n \rangle = \frac{1}{N} \qquad \langle c_m c_n \rangle = 0. \tag{25}$$

The expression for the WF (7) at some fixed position n can be rewritten in terms of *continuous* momentum variable $t = 2\pi m/N \in [0, 2\pi)$

$$W_{\psi,n}(t) = \sum_{q=-M}^{M} Z_q(n) \exp(\mathrm{i}qt) \qquad M = (N-1)/2. \tag{26}$$

Complex Fourier expansion coefficients Z_q are expressed in terms of state coefficients c_n

$$Z_q(n) = \frac{N}{\sqrt{N-1}} \sum_{l=-M}^{M} \tilde{\delta}(2l - 2n - q) c_{l-q} c_l^* \qquad Z_q^*(n) = Z_{-q}(n). \tag{27}$$

Now, the Fourier modes in (23) are simple bilinear functions of the coefficients c_n, namely

$$u_0 = Z_0 - \overline{W} \qquad u_q = Z_q + Z_q^* \qquad v_q = \mathrm{i}(Z_q - Z_q^*) \qquad q = 1, 2 \dots M. \tag{28}$$

By means of the central limit theorem one can argue in the asymptotic regime of large N, due to summation of statistically independent terms in equation (27), that u_n and v_n become (independent) Gaussian variables of vanishing first moments $\langle u_n \rangle = 0, \langle v_n \rangle = 0$. Straightforward but tedious calculation gives for the second moments

$$\langle u_q u_{q'} \rangle = \langle v_q v_{q'} \rangle = \frac{2}{N-1} \delta_{q,q'} \qquad \langle v_q u_{q'} \rangle = 0 \qquad \left\langle u_0^2 \right\rangle = \frac{1}{N-1}. \tag{29}$$

Therefore, the variances of Fourier coefficients are asymptotically, as $N \to \infty$, independent of the mode number q. This has also been verified by means of a numerical simulation of the WFL of random states, where c_n have been generated using a suitable random number generator. The results are shown in figure 11(*a*) where one sees excellent agreement with the prediction (29).

5.1.2. Random model on the sphere. All great circles on the sphere are statistically equivalent with respect to the WF (8) of a random state. Thus we choose to consider the equator $\theta = \pi/2$ for simplicity. Using the explicit expression for the spherical harmonics Y_{kq}

$$Y_{kq}(x) = N_{kq} P_k^q(\cos(\theta)) \exp(\mathrm{i}q\phi) \tag{30}$$

where N_{kq} are normalization constants and P_k^q are generalized Legendre polynomials, we have the explicit expression for the WF on the equator

$$W_\psi(\phi) = \sum_{q=-2J}^{2J} Z_q \exp(\mathrm{i}q\phi) \tag{31}$$

in terms of complex Fourier coefficients Z_q

$$Z_q = C_s \sum_{m,m'=-J} c_m c_{m'}^* K_{m,m'}^q$$

$$K_{m,m'}^q = \sum_{k=|q|}^{2J} N_{kq} P_k^q(0) \langle Jm'|T_{kq}^\dagger|Jm\rangle \in \mathbb{R}.$$

The coefficients Z_q are bilinear forms of wave coefficients c_m with the Gramm matrix $K_{mm'}^q$. The latter is difficult to evaluate explicitly. Using the symmetry of coefficients $Z_q = Z_{-q}^*$, we rewrite the WFL as

$$W_\psi(\phi) - \overline{W} = u_0 + \sum_{q=1}^{2J} u_q \cos(q\phi) + v_q \sin(q\phi) \tag{32}$$

where real Fourier coefficients are again simply related to complex coefficients Z_q by (28). The WF random model of spin J system has $M = 2J$ modes. In the semiclassical regime (large J) we can again show by means of the central limit theorem that u_q and v_q should be Gaussian distributed. Taking into account the detailed properties of terms in Z_q we can find the following statistical properties of u_q, v_q and u_0:

$$\langle u_q \rangle = \langle v_q \rangle = \langle u_0 \rangle = 0 \qquad \langle u_q v_{q'} \rangle = 0$$

$$\langle u_q u_{q'} \rangle = \langle v_q v_{q'} \rangle = \sigma_q^2 \delta_{q,q'} \qquad q = 1, \ldots, 2J.$$

The standard deviations of coefficients σ_q are essential for further discussion, but they are quite difficult to compute analytically. We, therefore, obtain them by numerical study of WFL for a random state. The results of numerical simulation are shown in figure 11(*b*). For large J, the results seem to be perfectly fitted by the *semicircle law*

$$\sigma_q^2 = \frac{2}{J\pi} \sqrt{1 - \left(\frac{q-1}{2J}\right)^2} \qquad q = 1, \ldots, 2J \tag{33}$$

which is conjectured to be the correct semiclassical limit.

5.2. Numerical study of the structure statistics of the Wigner function

Here we report on numerical simulations of the structure statistics of the WFL of time-dependent states in two classically chaotic quantum systems, namely of the quantized sawtooth map at $K_0 = 10$ on the torus, and the quantized kicked top at $\alpha = 10$, $\gamma = \pi/2$ on the sphere. In addition, we simulate for comparison the corresponding statistics for the appropriate random model discussed in the previous paragraphs, since these seem to be impossible to express analytically.

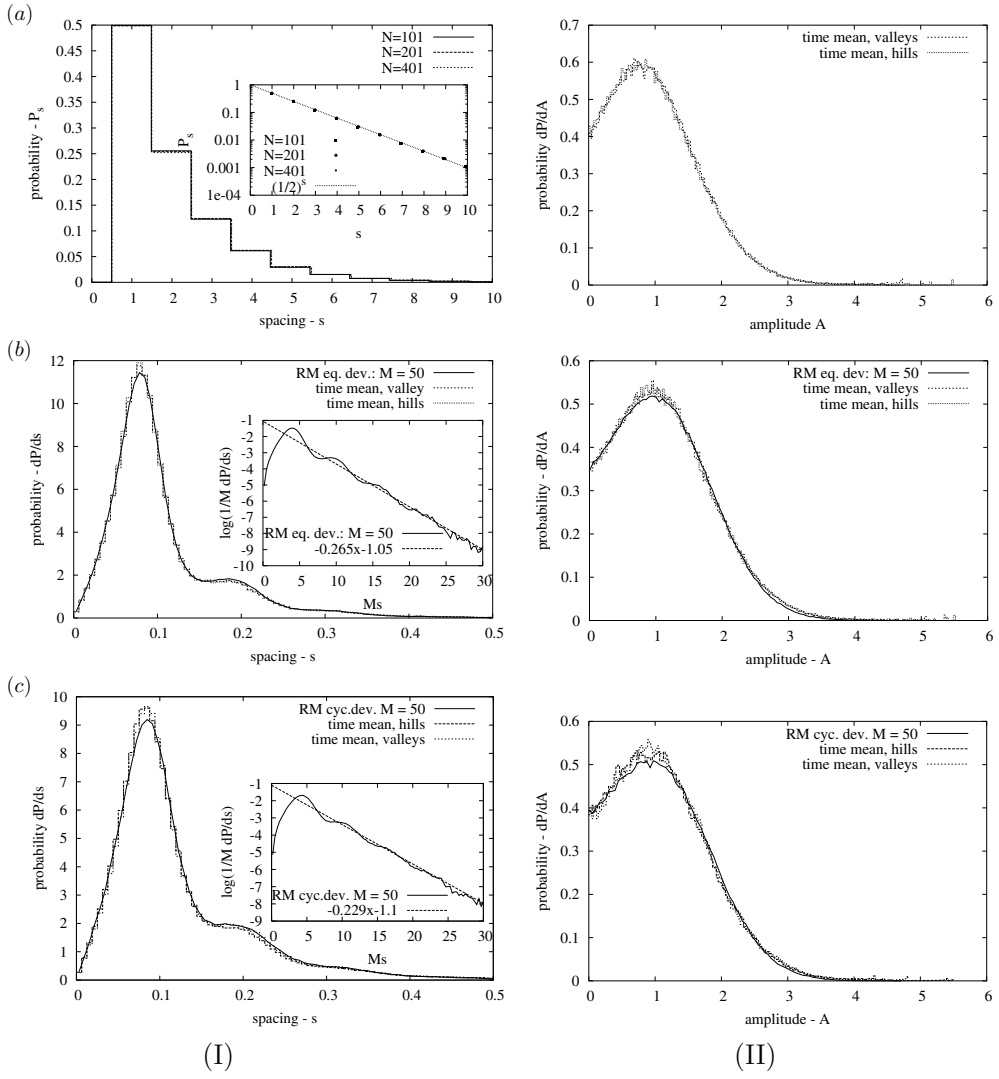

Figure 12. The average distribution of spacing s (I) and amplitude A (II) of the WF along a random line in phase space: (*a*) discrete torus (see text for explanation), (*b*) continuous torus, (*c*) sphere. In cases (*b*) and (*c*) the results of WFL simulations are compared with the results obtained from simulations of the random model (*RM*) for the specific geometry. In all examples we consider the case with $M = 50$ Fourier modes.

The results of our numerical studies of structure statistics $\mathrm{d}\mathcal{P}/\mathrm{d}s$, $\mathrm{d}\mathcal{P}/\mathrm{d}A$ and $\mathrm{d}\mathcal{P}/\mathrm{d}s\,\mathrm{d}A$ are shown in figure 12. Numerical experiments are done so that they correspond to the WF random model with $M = 50$. We can see good agreement between the random model and the numerical measurements on real dynamical systems. The latter are performed by time averaging over the evolution of an arbitrary initial state. We should stress that the numerical results are identical if we instead consider the Wigner function of a random (ergodic) state. With these results we have again shown, indirectly, that the assumptions in the derivation of the random model are correct. In the case of a spherical phase space there is a small deviation of

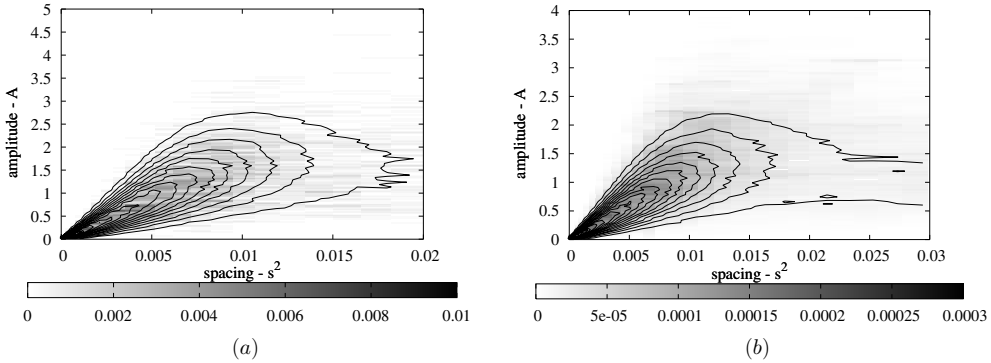

Figure 13. The average joint distribution of amplitude A and spacing s between two successive zeros of the WFL: (a) continuous torus, (b) sphere. For more details see the caption of figure 12. The density plot with greyness scales (indicated on the horizontal bar) refers to the simulation of true WFL, whereas isodensity contours refer to random models as discussed in the text.

the spacing distribution $\mathrm{d}\mathcal{P}/\mathrm{d}s$ around the peak of distribution due to imperfect approximation of the mode variances with the asymptotic semicircle formula (33).

The spacing distribution between neighbouring zeros $\mathrm{d}\mathcal{P}/\mathrm{d}s$ of the WFL (shown in figures 12(I)) gives some information on typical intersections of the nodal cells, whereas the amplitude distribution $\mathrm{d}\mathcal{P}/\mathrm{d}A$ (shown in figures 12(II)) gives information on the distribution of the heights in such intersected filaments. However, we note an interesting observation, namely that the statistics of the structure of positive nodal cells ($W - \overline{W} > 0$) is identical to the statistics of negative nodal cells ($W - \overline{W} < 0$) in the asymptotic regime $N \to \infty$. This is consistent with an asymptotic symmetric Gaussian distribution of Wigner function values (14). The spacing distribution exhibits periodically spaced peaks, with period π/M, and exponential tail with non-universal exponent for large s [23].

As the physical domain of the Wigner function on a torus is in fact a discrete mesh of $N \times N$ points, we also consider the statistics of a proper discrete WFL, namely $\widetilde{w}(m) = \widetilde{W}(2\pi m/N)$, and the discrete spacing distribution P_s which in fact measures the distribution of clusters of points where $\widetilde{w}(m)$ has constant sign, and the corresponding amplitude distributions. These are shown in figure 12(a). Interestingly, we find strong numerical evidence for the following exponential distribution:

$$P_s = 2^{-s}. \tag{34}$$

On the other hand, this is in fact just the distribution of the lengths of clusters of repeated uncorrelated binary events. This is consistent with the statement that the values of the WF of a random state on a physical quantum mesh of $N \times N$ phase-space points are indeed uncorrelated as suggested already by the auto-correlation function. We have also investigated the joint spacing–amplitude distributions $\mathrm{d}\mathcal{P}(s, A)/\mathrm{d}s\,\mathrm{d}A$, shown in figure 13. Again the results inferred from the simulations of the random model match the simulations of the WFL. We found that distributions $\mathrm{d}\mathcal{P}/\mathrm{d}s\,\mathrm{d}A$ have a simple shell-shaped form, indicating strong correlations between the spacing and the amplitude of the WF intersections. In fact one can give an upper bound on the maximally allowed amplitude A at a given small spacing s, namely this can be estimated from the second derivative (curvature) of the random model ansatz (23).

6. Summary and discussion

In this paper we have proposed studying statistical properties of Wigner functions of random pure quantum states, either eigenstates or time-dependent states of classically chaotic systems. We concentrated on the properties of quantum maps with 2D classical phase space. We have shown, using simple general arguments, that the Wigner function value distribution of a random state should tend to a Gaussian, in the semiclassical limit, which is centred around zero value, so the probabilities of having a negative or positive value become equal in the limit. In other words, the standard deviation divided by the mean value of the Wigner function diverges as $\sigma/\overline{W} \sim \sqrt{N}$ in the semiclassical limit $N \to \infty$. In addition, we have analysed the structure and phase-space correlations of Wigner functions of random states. In particular, we have shown that the auto-correlation of the Wigner function becomes a delta function in the semiclassical limit, and that the nodal cells have typical structures on the (sub-Planckian) scale $\delta q, \delta p \sim \hbar$.

We believe that our results may shed some new light on the related studies of decoherence [4, 22]. In particular, one now expects certain properties of the Wigner function of random states to be manifestly *non-classical*. For example, the fidelity of two initially equivalent states which undergo two slightly different time evolutions has been found to behave non-classically for times larger than the $-\log\hbar$ Ehrenfest time, i.e. when the states become effectively random, whereas the classical behaviour of fidelity has been recovered for shorter times [5]. We stress that we have in this study only considered non-autonomous (time-dependent, e.g. kicked) quantum systems, where Wigner functions of ergodic states are expected to occupy the entire classical phase space. On the other hand, one may ask similar questions about the statistics of Wigner functions on, or close to, energy surfaces of autonomous Hamiltonian systems. This is the subject of a forthcoming publication [25].

Acknowledgments

Useful discussions with A Backer, G Veble and M Žnidarič, as well as the financial support by the Ministry of Education, Science and Sport of Slovenia, are gratefully acknowledged.

References

[1] Wigner E 1932 On the quantum correction of thermodynamic equilibrium *Phys. Rev* **40** 749–59
[2] Berry M V 1977 Semiclassical mechanics in the phase space: a study of Wigner's function *Phil.Trans. R. Soc.* A **287** 237–71
[3] Voros A 1976 *Ann. Inst. H Poincaré* A **24** 31–90
Voros A 1977 *Ann. Inst. H Poincaré* A **26** 343–403
[4] Zurek W H 2001 Sub-Planck structure in phase space and its relevance for quantum decoherence *Nature* **412** 712–5
[5] Prosen T and Žnidarič M 2002 Stability of quantum motion and correlation decay *J. Phys. A: Math. Gen.* **35** 1455
[6] Karkuszewski Z P, Jarzynski C and Zurek W H 2002 Quantum chaotic environments, the butterfly effect, and decoherence *Phys. Rev. Lett.* **89** 170405
[7] Jacquod Ph, Adagideli I and Beenakker C W J 2002 Decay of the Loschmidt echo for quantum states with sub-Planck-scale structures *Phys. Rev. Lett.* **89** 154103
[8] de Groot S R and Suttorp L G 1972 *Foundations of Electrodynamics* (Amsterdam: North-Holland) ch VI
[9] Hannay J H 1998 The chaotic analytic function *J. Phys. A: Math. Gen.* **31** L755–61
[10] Nonnenmacher S and Voros A 1998 Chaotic eigenfunctions in phase space *J. Stat. Phys* **92** 431–518
[11] Agam O and Brenner N 1995 Semiclassical Wigner functions for quantum maps on a torus *J. Phys. A: Math. Gen.* **28** 1345–60

[12] Dowling J P, Agarwal G S and Schleich W P 1994 Wigner distribution of a general angular-momentum state: application to a collection of two-level atoms *Phys. Rev.* A **49** 4101–9
[13] Arecchi F T, Courtens E, Gilmore R and Thomas H 1972 Atomic coherent states in quantum optics *Phys. Rev.* A **6** 2211–37
[14] Agarwal G S 1981 Relation between atomic coherent-state representation, state multipoles, and generalized phase-space distributions *Phys. Rev.* A **24** 2889–96
[15] Kasperkovitz P and Peev M 1994 Weyl–Wigner formalisms for toroidal geometries *Ann. Phys., NY* **230** 21–51
Luis A and Peřina J 1998 Discrete Wigner function for finite-dimensional systems *J. Phys. A: Math. Gen* **31** 1423–41
de Almeida O and Rivas A M F 1999 The Weyl representation on the torus *Ann. Phys.* **276** 223–56
[16] Leboeuf P and Voros A 1990 Chaos-revealing multiplicative representation of quantum eigenstates *J. Phys. A: Math. Gen.* **23** 1765–74
[17] Edmonds A R 1974 *Angular Momentum in Quantum Mechanics* (Princeton, NJ: Princeton University Press)
[18] Benenti G and Casati G 2001 Sensitivity of quantum motion for classical chaotic systems *Preprint* quant-ph/0112060v1
[19] Haake F 1991 *Quantum Signatures of Chaos* (Berlin: Springer)
[20] Berry M V 1977 Regular and irregular wavefunctions *J. Phys. A: Math. Gen.* **10** 2083–91
[21] Bogomolny E, Bohigas O and Leboef P 1996 Quantum chaotic dynamics and random polynomials *J. Stat. Phys.* **85** 639–79
[22] Jordan A and Srednicki M 2001 Sub-Planck structure, decoherence, and many-body environments *Preprint* quant-ph/0112139v1
[23] Kuznetsov P L, Statonovich R L and Tikhonov V I 1954 On the duration of the exceedences of the random function *J. Tech. Phys. Moscow* **24** 103–12
[24] Berman G P and Zaslavsky G M 1978 Condition of stochasticity in quantum non-linear systems *Physica* A **91** 450
[25] Prosen T and Backer A 2002 in preparation